# Translational and rotational spectra in the fundamental infrared band of liquid and solid parahydrogen

A. Nucara, P. Calvani, S. Cunsolo, S. Lupi, and B. Ruzicka
*Dipartimento di Fisica, Università di Roma La Sapienza, 2, Piazzale Aldo Moro, 00185 Roma, Italy*
(Received 24 July 1992)

The $Q_1(0)$ and $Q_1(0)+S_0(0)$ infrared bands have been studied in liquid and solid para-$H_2$ with particular regard to their translational sidebands. In the liquid, their line shapes are well fitted by a model in which the excited particle is encapsulated. In the solid, the phonon sidebands reproduce the main features of the density of states (DOS), as extracted from neutron scattering. The $S_1(0)+S_0(0)$ band shows a pure rotonic line shape which is well described by recent DOS calculations.

## I. INTRODUCTION

Solid parahydrogen (para-$H_2$, $J$ even) and orthohydrogen (ortho-$H_2$, $J$ odd) are the simplest quantum crystals where molecular excitons are known to exist. Weak intermolecular interactions partially remove the crystal degeneracy, and allow the propagation of molecular excitonic modes.[1] Infrared absorption spectra which were attributed to propagating vibrons and rotons were indeed observed both in the vibrational fundamental band[2] of para-$H_2$ between 4000 and 5000 $cm^{-1}$, and in the pure rotational spectrum[3] between 300 and 600 $cm^{-1}$. The theoretical framework developed by Van Kranendonk[1] and by others[4–6] fully accounts for these observations.

In this paper we present detailed spectra of the fundamental band of para-$H_2$ for both the liquid and the solid phases. As its main features have been extensively studied since the work of Gush *et al.*,[2] our interest is focused on the translational sidebands of $Q_1(0)$ ($v=0\rightarrow v=1$, $J=0\rightarrow J=0$), $S_1(0)$ ($v=0\rightarrow v=1$, $J=0\rightarrow J=2$), and $Q_1(0)+S_0(0)$ ($v=0\rightarrow v=1$, $J=0\rightarrow J=0+v=0\rightarrow v=0$, $J=0\rightarrow J=2$). In the solid, such bands can be adequately described by admitting that photons are absorbed in processes where excitons and phonons are simultaneously excited. In the solid phase, the experimental spectral density $\Gamma(\nu)$ will be found in agreement with the phonon density of states (DOS) extracted from neutron scattering.[7,8] This picture will then be generalized, even if not strictly, to the liquid phase; in this case, the observed sidebands will be attributed to an encapsulated mode of the excited molecule within the cage of nearest neighbors. Contributions to the line shape from the quadrupole moments of residual ortho-$H_2$ impurities will also be taken into account. The above model yields good fits to the observed spectra. Nevertheless, the dominant frequency thus determined turns out to depend on the rotovibrational state of the molecule in a strong and presently unexplained way.

Finally, the $S_1(0)+S_0(0)$ infrared band is resolved and studied. It is interesting in that its spectrum does not contain any contribution from propagating vibrational excitons. The observed line shape of $S_1(0)+S_0(0)$ is then closely related to the roton density of states, and indeed it agrees well with the calculated[5] structure of the latter.

## II. EXPERIMENT

The infrared spectra reported here were collected by condensing samples of para-$H_2$ in a suitably modified Oxford Instruments variable temperature cryostat. Three Pyrex cells, having optical lengths of 22, 11, and 1 mm, were employed. Temperature was controlled by heaters driven by two sensors: a germanium thermometer placed on the wall of the cell, and a Rh-Fe resistor in the He gas. Temperature was kept stable—and measured—within 0.2 K. Spectra at 2 K were collected with the cell fully immersed in superfluid helium.

Parahydrogen was prepared by converting normal liquid $H_2$ with the help of a suitable catalyst ($Cr_2O_3$-$\gamma Al_2O_3$). The para-$H_2$ sample was then evaporated and recondensed into the cryostat, where solid samples were grown by slowly cooling the liquid. In such a way, optically transparent crystals were finally obtained. Thin polycrystalline layers were observed at the center of the windows in the 22 mm samples only. Residual ortho-$H_2$ impurities, possibly produced during evaporation and recondensation, were found in the para-$H_2$ crystals. Their final concentration was extracted from the measured integrated absorption coefficient of the $Q_1(0)$ quadrupolar band, which appears as a narrow line in the absorption spectrum of the thickest sample reported in Fig. 1. By comparison with theory[9] in the limit of low ortho concentration, we estimated that this latter never exceeded (5±1)% for the spectra reported in this paper. We can evaluate that a few residual ortho molecules do not appreciably affect the present study of para-$H_2$ behavior, as also shown by the observation in the solid phase of spectral details that had been previously reported for the purest samples.[2] As it will be shown in the following, the quadrupolar contribution to $\Gamma(\nu)$ due to ortho-$H_2$ impurities has been taken into account, and subtracted. On the other hand, the observation of ortho-$H_2$ weak spectral features facilitates calibration procedures and line assignment.

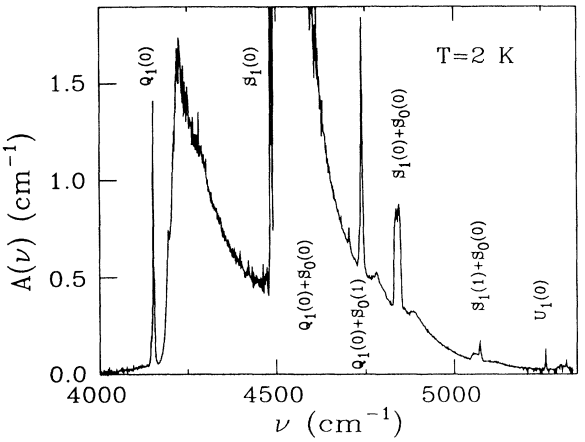


FIG. 1. The absorption spectrum at 2 K of a solid para-$H_2$ sample having a thickness of 22 mm. The apodized resolution is 0.7 cm$^{-1}$. The $Q_1(0)+S_0(1)$, $S_1(1)+S_0(0)$ lines are due to residual ortho-$H_2$ impurities, while $U_1(0)$ corresponds to a $v=0 \rightarrow v=1$, $J=0 \rightarrow J=4$ transition.

Infrared transmission spectra were collected by using a rapid scanning interferometer with a maximum resolution of 0.7 cm$^{-1}$. The observed spectra were corrected for the reflectivity of the cell by comparing the transmittance of samples with thicknesses of 11 and 22 mm. Then, the absorption coefficient $A(\nu)$ defined as

$$A(\nu)=\frac{\eta}{d}\ln\left(\frac{I_0(\nu)}{I(\nu)}\right) \tag{1}$$

was obtained, where $I(\nu)$ is the radiation intensity transmitted by the sample, $I_0(\nu)$ is the background intensity transmitted by the empty cell, $d$ is the sample thickness, and $\eta$, the Polo-Wilson factor,[10] takes into account the effect of the local field on a single molecule.

In absorption spectroscopy it is often convenient to introduce the spectral density or line shape $\Gamma(\nu)$ and the reduced line shape $G(\nu)$, which are related to the absorption coefficient through the relations

$$\Gamma(\nu)=\frac{1}{\nu}A(\nu)[1-\exp(-\beta h\nu c)]^{-1} \tag{2}$$

with $\beta=\frac{1}{kT}$, and

$$G(\nu)=\tfrac{1}{2}[\Gamma(\nu)+\Gamma(-\nu)]. \tag{3}$$

The line shape $\Gamma(\nu)$ satisfies the detailed balance principle:

$$\Gamma(-\nu)=\exp(-\beta h\nu c)\Gamma(\nu). \tag{4}$$

## III. RESULTS AND DISCUSSION

### A. $Q_1(0)$ band in liquid para-$H_2$

A typical example of line shape $\Gamma(\nu)$ of para-$H_2$ in the $Q_1(0)$ region, as measured in the liquid phase, is reported in Fig. 2. The figure shows two main features: a broadband peaked at about 4240 cm$^{-1}$ and a narrow one centered at 4154.2 cm$^{-1}$. The former is induced by the isotropic overlap of vibrating para-$H_2$ molecules, while the latter is induced by the quadrupole moments of residual ortho-$H_2$ neighbors. As the effective induction range is longer for the quadrupolar induction mechanism, the quadrupolar band is much narrower than that due to overlap.

The quadrupolar contribution to $Q_1(0)$ may be easily subtracted, and the overlap term obtained. We can assume that the vibrational frequency $\nu_{1,0}$ coincides with the peak frequency of the $Q_1(0)$ quadrupolar line and we neglect the coupling between translation and vibration in liquid $H_2$. We can then express the overlap contribution to $\Gamma(\nu)$ as the product of a translational factor $\Gamma_\mu(\nu-\nu_{1,0})$ and the squared matrix element of the amplitude of the dipole moment between the ground state and the $n=1$ state, where $n$ is the vibrational quantum number:

$$\Gamma(\nu)=\Gamma_\mu(\nu-\nu_{1,0})\mu_{1,0}^2. \tag{5}$$

Thus from the measured spectrum a quantity proportional to $\Gamma_\mu(\nu-\nu_{1,0})$ is deduced, and the translational reduced line shape $G_\mu(\nu-\nu_{1,0})$ is extracted.

Figure 3 shows a typical example of the translational reduced line shape $G_\mu(\Delta\nu)$, with $\Delta\nu=\nu-\nu_{1,0}$. In the low-frequency region $G_\mu(\Delta\nu)$ exhibits a dip. This is a characteristic density effect induced by isotropic overlap on the translational bands. It has been observed in $H_2$–noble-gas mixtures both in the high density gaseous phase and in the liquid phase.[11] The low-frequency dip in $G_\mu(\Delta\nu)$ is due to the interference between dipoles induced in successive repulsive interactions of the inducing particle with the medium.[12] Therefore, it is often called the *intercollisional interference effect* (IIE).

The isotropic overlap induction mechanism is usually active in a pair of unlike and interacting atoms or molecules. Nevertheless, it may also be observed in a pair of interacting molecules which belong to the same chemical species and are in different vibrational states. This is just the case of the overlap component observed

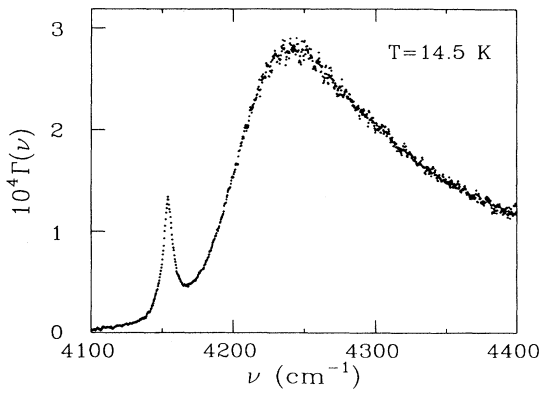


FIG. 2. The spectral density $\Gamma(\nu)$ of liquid para-$H_2$ in the $Q_1(0)$ region at 14.5 K.

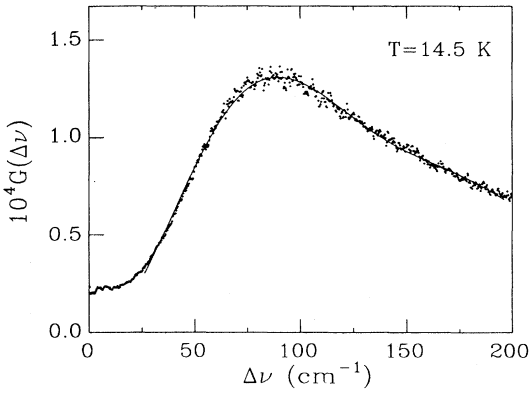


FIG. 3. The reduced line shape $G(\Delta\nu)$ in liquid para-$H_2$ at 14.5 K (dots). The solid line is the best fit obtained from Eq. (6).

here in the $Q_1(0)$ of para-$H_2$. A molecule in the $n = 1$ vibrational state may be regarded as an impurity, moving in a medium of para-$H_2$ molecules in their ground state. The occurrence of IIE may be qualitatively explained by assuming that the dipole moment $\boldsymbol{\mu}(R)$ and the force $\mathbf{F}(R)$ associated with the vibrating molecule are simply proportional. Then, $G_\mu(\Delta\nu)$ is proportional to $G_F(\Delta\nu)$. Moreover, on the basis of general arguments,[11] $G_F(\Delta\nu) \to 0$ as $D(\Delta\nu)^2$, with $D$ the diffusion coefficient, as $\Delta\nu \to 0$. Consequently also $G_\mu(\Delta\nu)$ approaches zero when $\Delta\nu$ vanishes.

The validity of the assumption $\boldsymbol{\mu}(R) \propto \mathbf{F}(R)$ at liquid densities is still an open question. From molecular dynamics computations we may conclude that even if $\boldsymbol{\mu}(R)$ and $\mathbf{F}(R)$ are not exactly proportional, the correlation functions $C_\mu(t)$ and $C_F(t)$ are similar in shape[13] and $G_\mu(\Delta\nu)$ has, anyway, a low frequency dip.[14] Data reported in Fig. 3 clearly show the occurrence of IIE, and also show that $G_\mu(\Delta\nu)$ does not vanish when $\Delta\nu = 0$. This indicates that $\boldsymbol{\mu}(R)$ and $\mathbf{F}(R)$ are not exactly proportional.[12] Nevertheless the shape of $G_\mu(\Delta\nu)$ in Fig. 3 is quite similar to that observed for noble gases dissolved in liquid Ar.[15] The translational reduced line shapes in liquid mixtures have been analyzed by using the profile[15]

$$G_\mu(\Delta\nu) = A\left(\frac{\Delta\nu}{\nu_0}\right)^2 \frac{2X(\Delta\nu)}{\{[X(\Delta\nu)]^2 + [2\pi c\,\Delta\nu - Y(\Delta\nu)]^2\}}, \tag{6}$$

where

$$X(\Delta\nu) = (2\pi^2\nu_0^2\sqrt{\pi}\tau)\exp[-(\pi c\tau\,\Delta\nu)^2][1 + \varepsilon H_4(\pi c\tau\,\Delta\nu)], \tag{7}$$

$$Y(\Delta\nu) = -4\pi^2\nu_0^2\tau\exp[-(\pi c\tau\,\Delta\nu)^2][1 + \varepsilon H_4(\pi c\tau\,\Delta\nu)]\int_0^{\pi c\tau\,\Delta\nu}\exp(y^2)dy - 4\varepsilon\pi^2\nu_0^2\tau[\tfrac{5}{4}\pi c\tau\,\Delta\nu - \tfrac{1}{2}(\pi c\tau\,\Delta\nu)^3], \tag{8}$$

and $A = 0.58$ cm$^{-1}$.

The above expressions contain the parameters $\nu_0, \tau$, and $\varepsilon$. A particle in a liquid undergoes a motion which is both encapsulated and diffusive.[16] The frequency $\nu_0$ characterizes the encapsulated contribution to the motion of the inducing molecule with respect to the cage of nearest neighbors. In turn, $\tau$ parametrizes the exponential decay of the autocorrelation function $M(t)$ and it is related both to the second moment $\gamma_2$ and to the zero moment $\gamma_0$ of $G_\mu(\Delta\nu)$ by the relation

$$\tau = \sqrt{\frac{2\gamma_0}{(\gamma_2 - 4\pi^2\gamma_0\nu_0^2)}}. \tag{9}$$

Finally, $\varepsilon$ may be related to the fourth moment of $G_\mu(\Delta\nu)$. The solid line in Fig. 3 is obtained by fitting Eq. (6) to the experimental $G_\mu(\Delta\nu)$. The fit gives $\nu_0 = 114$ cm$^{-1}$, $\tau = 1.04 \times 10^{-13}$ sec, and $\varepsilon = 0.23$. It is reasonable to assume that when passing from the liquid to the solid phase the parameter $\nu_0$ becomes the average of the frequencies in the Brillouin zone so that it can be assumed to be of the same order as the Debye frequency in the solid. In para-$H_2$ one extracts $\nu_D = 88$ cm$^{-1}$ from the velocity of sound,[17] in qualitative agreement with the value of 114 cm$^{-1}$ found here for $\nu_0$ .

### B. $Q_1(0)$ band in the solid phase

The line shape $\Gamma(\nu)$ of a solid para-$H_2$ sample with about 4% ortho-$H_2$ is reported in Fig. 4 for the $Q_1(0)$ region. In analogy with the liquid phase, both a quadrupolar line peaked at 4152.8 cm$^{-1}$ and a broadband are detected. The latter is induced by the isotropic overlap associated with the vibrating para-$H_2$ molecule, and arises from transitions to the $n = 1$ exciton state involving the emission of phonons.[2] The quadrupolar line has been extensively studied[2,9] and the values of the integrated absorption coefficient, as mentioned above, have been used here to obtain a careful estimation of the ortho-$H_2$ concentration.

Four features can be identified in the phonon branch. The weak contributions at $\nu_a$ =43.5 cm$^{-1}$ and $\nu_b$ =58.5 cm$^{-1}$ from the strongest quadrupolar line (which is assumed as zero frequency in the inset) are both meaningful due to the low noise level[18] at those frequencies. In addition, one has the strong and broad peak centered at $\nu_c$ =75.0 cm$^{-1}$, and what seems to be a two-phonon replica of $\nu_c$, at $\nu_d$ =145 cm$^{-1}$.

Phonon peaks at frequencies which correspond within errors to $\nu_a$ have been observed in the sidebands of $U_0(0)$ and $U_0(1)$ by Balasubramanian *et al.*,[19] and in the first

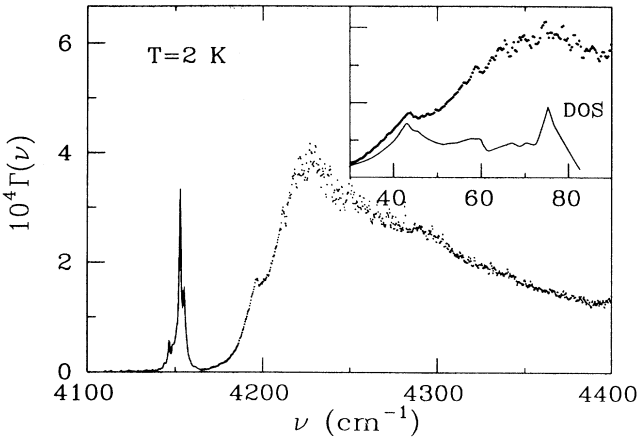


FIG. 4. The spectral density $\Gamma(\nu)$ for solid para-$H_2$ in the $Q_1(0)$ region. In the inset, the dots are experimental data, the solid line is the phonon density of states (DOS) as calculated in Ref. 7.

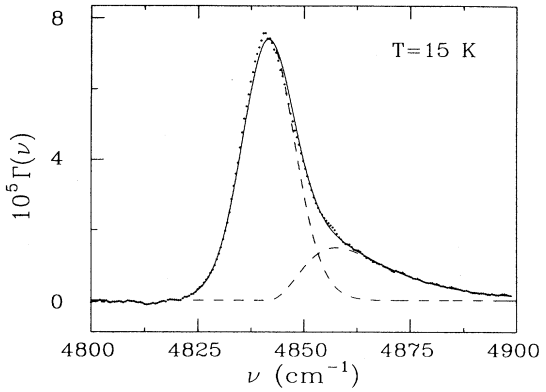


FIG. 5. The spectral density $\Gamma(\nu)$ of liquid para-$H_2$ at 15 K in the $S_1(0)+S_0(0)$ region (dots) is compared with the results of the fit. The solid line is the sum of $\Gamma_t$ and $\Gamma_r$ as obtained from Eqs. (12) and (11), respectively (dashed lines).

vibrational overtone by Varghese, Prasad, and Reddy.[20] A comparison can also be made between our data and the calculated density of phonon states. Indeed, $\Gamma(\nu)$ for a phonon branch involving the emission of a single phonon may be represented by an expression of the form

$$\Gamma(\nu) \propto |\mu^{\rm ph}(\nu)|^2 \rho(\nu), \tag{10}$$

where $\mu^{\rm ph}(\nu)$ is the matrix element of the dipole moment and $\rho(\nu)$ is the DOS for lattice vibrations. Higher values of $\nu$ will correspond to greater relative displacements of neighboring molecules, and hence to greater changes in the dipole moment. Then one expects $|\mu^{\rm ph}(\nu)|^2$ to be a smooth function of $\nu$, and one can attribute the peaks in $\Gamma(\nu)$ to corresponding maxima in the density of states $\rho(\nu)$.

Equation (10) holds up to a maximum frequency $\nu_{\rm max}$ which approximately corresponds to the Debye frequency $\nu_D$. Since $\nu_c$ turns out to be close to $\nu_D$, we can identify $\nu_c$ with $\nu_{\rm max}$. Moreover, $\nu_a$, $\nu_b$, and $\nu_c$ as shown in the inset of Fig. 4 are in very good agreement with the positions of the peaks in the density of state $\rho(\nu)$, as derived from neutron scattering experiments.[7,8] In particular, $\nu_a$ corresponds to a transverse optical mode at the $\Gamma$ point.[8]

The $\Gamma(\nu)$ tail above $\nu_{\rm max}$ arises from multiphonon processes and is quite similar in shape to the tail of the overlap component of $Q_1(0)$ in the liquid phase reported in Fig. 2. In both cases the main contribution to $\Gamma(\nu)$ arises from the dipole moment induced between molecules at a very short distance and it is almost unaffected by the surrounding medium. The feature at $\nu_d \approx 2\nu_{\rm max}$ is present in the solid phase only and is probably due to two-phonon processes.

The integrated absorption coefficient of the $Q_1(0)$ phonon branch has also been derived, in spite of difficulties arising from the superposition of the tail of $S_1(0)$ with the $Q_1(0)+S_0(0)$ sideband. For $\nu > 4400$ cm$^{-1}$, the spectrum was corrected by using a fit based on Eq. (6). We finally obtained $\tilde{\alpha} = (0.79 \pm 0.02) \times 10^{-13}$ cm$^3$ sec$^{-1}$, in good agreement with the value $\tilde{\alpha} = 0.7 \times 10^{-13}$ cm$^3$ sec$^{-1}$ reported in Ref. 9.

### C. $S_1(0)+S_0(0)$ band in liquid para-$H_2$

The line shape $\Gamma(\nu)$ of para-$H_2$ in the $S_1(0)+S_0(0)$ region, as measured in the liquid phase, is reported in Fig. 5. The concentration of ortho-$H_2$ was estimated to be about 4%. The figure suggests that $\Gamma(\nu)$ arises from the superposition of two contributions, a line with a width of about 20 cm$^{-1}$ and a tail at higher frequencies. The first contribution is centered at $\nu_a$=4841.7 cm$^{-1}$ which corresponds exactly to the sum of the frequency (355.7 cm$^{-1}$) of the $k = 0$ rotational exciton[3] $S_0(0)$ and to the one (4486.0 cm$^{-1}$) of the rotovibrational exciton[2] $S_1(0)$. We interpreted the first contribution as due to an $S_1(0)$ localized transition associated with a rotational $S_0(0)$ transition in the surrounding medium [i.e., an $S_1(0)+S_0(0)$ transition]. We interpreted the tail as due to a process involving both an $S_1(0)+S_0(0)$ transition and a change of the translational state of the system. Similar processes take place in the phonon branches of the solid. We describe the first contribution with a modified Gaussian

$$\Gamma_r(\Delta\nu) = A_r \exp[-(\pi c \tau_r \Delta\nu)^2][1 + \varepsilon_r H_4(\pi c \tau_r \Delta\nu)] \tag{11}$$

with $\Delta\nu = \nu - \nu_a$. We described instead the second contribution, involving changes in the translational energy, with the empirical function

$$\Gamma_t(\Delta\nu) = A_t[1 - \alpha_t \exp(-\Delta\nu/\nu_t)^2] \exp[-(\pi c \tau_t \Delta\nu)^2][1 + \varepsilon_t H_4(\pi c \tau_t \Delta\nu)] \tag{12}$$

when $\Delta\nu \geq 0$, while at low temperature we may assume $\Gamma_t(\Delta\nu) = 0$ when $\Delta\nu \leq 0$. The solid line in Fig. 5 represents the best fit of the profiles (11) and (12) to the experimental data, as obtained by choosing the parameters $A_r = 8.2 \times 10^{-5}$, $\tau_r = 1.16 \times 10^{-12}$ sec, $\varepsilon_r = 3.65 \times 10^{-2}$, $A_t = 2.34 \times 10^{-5}$, $\alpha_t = 1.0$, $\nu_t = 11$ cm$^{-1}$, $\tau_t = 3.07 \times 10^{-13}$ sec, and $\varepsilon_t = 0.15$. The widths of $\Gamma_r(\Delta\nu)$ and $\Gamma_t(\Delta\nu)$ imply different relaxation times $\tau_r$ and $\tau_t$ and suggest that the two bands are due to quadrupolar and overlap induction mechanisms, respectively.

The above analysis is not dissimilar from the one reported for the $Q_1(0)$ band in a previous section. However, as the processes which determine $\Gamma_t(\Delta\nu)$ in Fig. 5 also involve the creation of a rotational excitation in the liquid, they are more complicated than those responsible for $G_\mu(\Delta\nu)$ in Fig. 3.

### D. $S_1(0)+S_0(0)$ band in solid para-$H_2$

The line shape of para-$H_2$ in the $S_1(0)+S_0(0)$ region, as measured in the solid phase at $T = 2$ K, is reported in Fig. 6. There also the line shape can be described as produced by the superposition of a quadrupolar contribution and of a phonon branch. The former includes an $S_1(0)$ localized exciton and an $S_0(0)$ roton, freely propagating in the solid. As expected, the resulting line shape is somewhat different from that of the corresponding band in $Q_1(0)+S_0(0)$. In the latter, the peaks arise from the maxima in the vibron-roton joint density of states (JDOS), while in the $S_1(0)+S_0(0)$ band the peaks correspond to the maxima of the roton DOS only. The roton DOS in para-$H_2$ has been calculated by Bose and Poll.[5] As shown in the inset of Fig. 6, it is found in excellent agreement with our results if the zero energy is placed at 4838.5 cm$^{-1}$, a value which differs by about 3 cm$^{-1}$ from the sum of the unperturbed frequencies of $S_1(0)$ and $S_0(0)$.

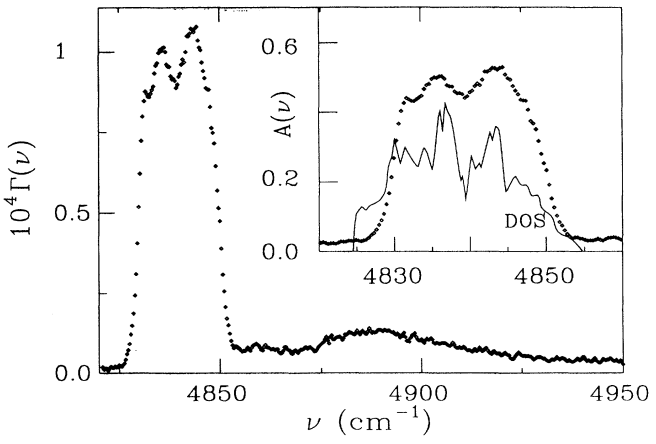


FIG. 6. The spectral density $\Gamma(\nu)$ in the $S_1(0) + S_0(0)$ region for solid para-$H_2$ at 2 K. The absorption coefficient $A(\nu)$ of the roton band is reported in cm$^{-1}$ in the inset, and compared therein with the density of states (DOS) calculated in Ref. 5. The zero shift of the DOS profile is assumed to be at 4838.5 cm$^{-1}$.

A less satisfactory agreement is provided by the calculated spectrum[6] of $S_v(0)+S_0(0)$, not shown in Fig. 6.

Finally we point out that the phonon branch of the solid seems to extend at frequencies higher than the translational band in the liquid. A peak is found at about 47 cm$^{-1}$ from the sum of the frequencies corresponding to $S_1(0)$ and to $S_0(0)$.

### E. $S_1(0)$, $Q_1(0)+S_0(0)$ band

The line shape in the $S_1(0)$ and $Q_1(0)+S_0(0)$ region is shown in Fig. 7 for solid para-$H_2$ at 2 and 11 K, and for liquid para-$H_2$ at $T = 14.5$ K. The $S_1(0)$ band, which corresponds to a localized rotovibrational exciton, is completely absent in the liquid phase due to the cancellation effect. On the other hand, both in the liquid and in the solid at 11 K, $Q_1(0)+S_0(0)$ exhibits a well-defined maximum at about 4505.5 cm$^{-1}$, a value obtained by summing the frequencies of a roton and a vibron[2] at $k = 0$.

In analogy with the $S_1(0)+S_0(0)$ band, previously considered, $\Gamma(\nu)$ can be interpreted as the sum of two contributions: a pure $Q_1(0)+S_0(0)$ component $\Gamma_{Qr}$ and a translational component $\Gamma_{Qt}$. In the liquid, $\Gamma_{Qt}$ may be described by the empirical function (12) previously introduced, where however $\Delta\nu = \nu - \nu_b$ is now referred to a frequency $\nu_b$ which coincides with that of the $S_1(0)$ excitonic line in the solid. We found out that the $\Gamma_{Qr}$ component is no longer described by Eq. (11), while it may be well reproduced by the Lorentzian:

$$\Gamma_{Qr}(\Delta\nu) = \frac{A_r}{(\Delta\nu)^2 + \gamma^2}, \tag{13}$$

where $\gamma$ is the half-width. The solid line in Fig. 7 represents the best fit to data of the profiles $\Gamma_{Qr}$ and $\Gamma_{Qt}$, as given by Eqs. (13) and (12), respectively. Dashed lines represent their separate contributions, and one can notice that $\Gamma_{Qr}$ in Fig. 7 has the same width within errors as the corresponding quantity $\Gamma_r$ reported in Fig. 5. In the solid at 2 K, the $Q_1(0)+S_0(0)$ line shape confirms previous observations[2] and will not be further analyzed

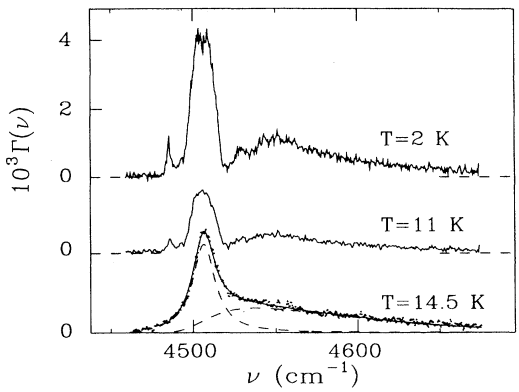


FIG. 7. The spectral density $\Gamma(\nu)$ for the $S_1(0)$, $Q_1(0) + S_0(0)$ band in solid para-$H_2$ at 2 and 11 K, and in liquid para-$H_2$ at 14.5 K. The samples had a thickness of 1 mm.

here.

As far as the translational band is concerned, its line shape $\Gamma_{Qt}$ exhibits at 2 K two peaks at 44 and 66 $cm^{-1}$ from the $S_1(0)$ line. The assignment of the observed phonon branch to $S_1(0)$ is justified by the fact that this latter is expected to be twice as intense as the $Q_1(0)+S_0(0)$ phonon branch.[4] The two phonon peaks rapidly broaden and in the liquid phase they turn into a band with a maximum at $\Delta\nu_l = 50$ $cm^{-1}$. This value may again roughly measure the characteristic frequency of an encapsulated motion.

## IV. CONCLUSION

In this paper we have analyzed the fundamental rotovibrational band of solid and liquid para-$H_2$ with low residual ortho concentration. With respect to previous experiments,[2,20] the interest has been focused here on the translational sidebands and on the $S_1(0)+S_0(0)$ band, which has been studied in detail.

In the solid phase, phonon contributions peaked at 43, 58, and 75 $cm^{-1}$ have been found in the $Q_1(0)$ band. These values are in good agreement with those (47, 55, and 67 $cm^{-1}$) measured for the $S_0(0)$ band[3] in the far infrared and correspond to three peaks in the calculated density of phonon states.[7] In the $S_1(0)$, $Q_1(0)+S_0(0)$ band two phonon peaks have been detected at 44 and 66 $cm^{-1}$. These results show that the phonon frequencies of para-$H_2$ are independent within errors of the particular excitonic transition they are associated with.

For the liquid phase, a procedure aimed at extracting physical information from the infrared sidebands has been developed. In particular, the dominating frequency $\nu_0$ of an excited para-$H_2$ molecule which moves in the cage produced by its nearest neighbors has been evaluated. Indeed, the cage can be assumed to be stable on this time scale, as its lifetime is comparable with the times characteristic of diffusion processes. Different values have been obtained for $\nu_0$: we have found 50 $cm^{-1}$ for the $S_1(0)$, $Q_1(0)+S_0(0)$ band, 114 $cm^{-1}$ for the $Q_1(0)$ band, while a peak in the translational band associated with the $S_0(0)$ transition was found in the far infrared at 37 $cm^{-1}$.[3] Such discrepancies may be partially explained by considering that the interaction potential between an excited para-$H_2$ molecule and the surrounding medium depends on its rotovibrational state.

Finally, the $S_1(0)+S_0(0)$ band has been resolved and studied in detail. It offers the opportunity to observe a roton band without any contribution from propagating vibrons. We have found that the $S_0(0)$ line shape reproduces quite well the features of the calculated[5] roton density of states. In a forthcoming paper, the analysis presented here will be extended to the spectral region of the first overtone of parahydrogen.


[1] J. Van Kranendonk, *Solid Hydrogen* (Plenum, New York, 1983).

[2] H. P. Gush, W. F. Hare, E. J. Allin, and H. L. Welsh, Can. J. Phys. **38**, 1495 (1960).

[3] U. Buontempo, S. Cunsolo, P. Dore, and L. Nencini, Can. J. Phys. **60**, 1422 (1982).

[4] J. D. Poll and J. Van Kranendonk, Can. J. Phys. **40**, 163 (1961).

[5] S. K. Bose and J. D. Poll, Can. J. Phys. **68**, 159 (1990).

[6] K. Morishita and J. Igarashi, J. Phys. Soc. Jpn. **58**, 3406 (1989).

[7] K. Carneiro and M. Nielsen, in *Anharmonic Lattices, Structural Transitions and Melting*, edited by T. Riste (Nordhoff, Leiden, 1974).

[8] M. Nielsen, Phys. Rev. B **7**, 1626 (1973).

[9] V. F. Sears and J. Van Kranendonk, Can. J. Phys. **42**, 980 (1964).

[10] J. Van Kranendonk, Physica **23**, 825 (1957).

[11] W. F. Hare and H. L. Welsh, Can. J. Phys. **36**, 88 (1957); S. Cunsolo and H. P. Gush, *ibid.* **50**, 2058 (1972); A. R. W. McKellar, J. W. MacTaggart, and H. L. Welsh, *ibid.* **53**, 2060 (1975).

[12] J. Van Kranendonk, in *Proceedings of the International School of Physics "Enrico Fermi"* Course LXXV, edited by J. Van Kranendonk (North-Holland, Amsterdam, 1978), p. 77; J. C. Lewis, *ibid.* p. 94; J. Van Kranendonk, Can. J. Phys. **46**, 1173 (1968).

[13] S. Weis, H. L. Strauss, and B. J. Alder, Mol. Phys. **38**, 1749 (1979); J. C. Lewis and J. A. Tjon, Physica A **91**, 161 (1978).

[14] G. Birnbaum and R. D. Mountain, J. Chem. Phys. **81**, 2347 (1984).

[15] U. Buontempo, P. Codastefano, S. Cunsolo, P. Dore, and P. Maselli, Can. J. Phys. **59**, 1495 (1981).

[16] U. Buontempo, S. Cunsolo, P. Dore, and P. Maselli, in *Intermolecular Spectroscopy and Dynamical Properties of Dense Systems*, Proceedings of the International School of Physics "Enrico Fermi" Course LXXV, edited by J. Van Kranendonk (North-Holland, Amsterdam 1978), p. 211.

[17] R. D. McCarty, J. Hord, and H. M. Roder (unpublished).

[18] The abrupt increase of the noise on the top of the phonon branch, see also Fig. 2, is related to a limited sensitivity of both the mercury-cadmium-tellurium detector and the ADC of the interferometer, for nearly saturated absorption.

[19] T. K. Balasubramanian, Chen Hsin-Lien, K. Narahari Rao, and J. R. Gaines, Phys. Rev. Lett. **47**, 127 (1981).

[20] G. Varghese, R. D. G. Prasad, and S. P. Reddy, Phys. Rev. A **35**, 701 (1987).